Growth and structural characterization of Ni/Co superlattices

J. M. Gallego, S. Kim, T. J. Moran, D. Lederman, and Ivan K. Schuller
Department of Physics 0319, University of California–San Diego, La Jolla, California 92093-0319
(Received 19 September 1994)

Ferromagnetic/ferromagnetic Ni/Co superlattices have been grown by molecular-beam epitaxy on $Al_2O_3(11\bar{2}0)$ substrates. X-ray diffraction and surface analysis techniques (low-energy electron diffraction and Auger-electron spectroscopy) show that the superlattices grow epitaxially, both Ni and Co in the fcc structure, and with the (111) direction normal to the surface. The superlattices are single crystalline in the growth direction, have an approximately square chemical modulation wavelength, and show four different types of in-plane domains. The lattice parameters measured in the (111) direction are consistent with Co and Ni maintaining their bulk lattice parameters. In the plane of the superlattice, the two materials are lattice matched.

Magnetic multilayers and superlattices have received much attention recently from both the fundamental and technological points of view. Besides their potential applications as magnetic sensors and media, these systems attract much interest because of the novel and exotic properties they exhibit when compared to the bulk properties of their constituents.[1–3] These properties include, but are not limited to, giant magnetoresistance,[4] oscillatory coupling,[5] and perpendicular magnetic anisotropy.[6] Also, magnetic multilayers provide the possibility to study physical phenomena, such as magnetism or superconductivity, in low-dimensional systems, or to stabilize new phases of magnetic materials.

A complete understanding of these new physical and chemical properties, however, requires a thorough knowledge of the multilayer structure, as many of these properties strongly depend on structural characteristics such as crystallinity, grain size, roughness, interdiffusion, and strain. As an example, the study of two-dimensional magnetism implies the necessity of growing multilayers with small magnetic layer thicknesses of a known structure and a square modulation wavelength, as the interdiffusion of the magnetic atoms with the neighboring layers can greatly affect their magnetic properties.

Until now, most of the work on magnetic metallic superlattices has been focused on those where only one of the two materials is ferromagnetic, the other being nonmagnetic or antiferromagnetic. These systems allow the study, for example, of the type of coupling between magnetic layers separated by nonmagnetic materials. Magnetic metallic multilayers where both materials are ferromagnetic have been much less studied, although they exhibit some interesting properties, such as oscillatory behavior of the transport properties as a function of the Ni thickness,[7] large magnetoresistances with low saturation fields[8] and perpendicular magnetic anisotropy[9] in Ni/Co superlattices, stabilization of bcc Co in Fe/Co multilayers,[10] and stabilization of fcc Fe in Fe/Ni multilayers.[11]

In this paper, we report on the growth and structural characterization of Ni/Co superlattices on $Al_2O_3(11\bar{2}0)$. A combination of *in situ* surface analysis techniques and *ex situ* x-ray diffraction has been used to gain insight into the chemical and structural order of the superlattices. We show that high-quality epitaxial Ni/Co superlattices can be prepared with a perpendicular coherence length of $\sim$ 1000 Å, both Ni and Co growing in the fcc structure, with the (111) direction normal to the superlattice surface, and lattice matched in the plane. Although the magnetic properties of Ni/Co superlattices have been studied previously,[7–9,12] to our knowledge no detailed structural characterization has ever been reported.

The $(Ni_a/Co_b)_N$ superlattices (where a and b are the thicknesses in Å of the Ni and Co layers, respectively, and N is the total number of bilayers), were grown on sapphire substrates $[Al_2O_3(11\bar{2}0)]$ by molecular-beam epitaxy (MBE) in an ion-pumped Riber MBE system equipped with a 10 keV electron gun for reflection high-energy electron diffraction (RHEED), a four-grid optics with a coaxial electron gun for low-energy electron diffraction (LEED) and Auger electron spectroscopy (AES), and a quadrupole residual gas analyzer. The base pressure was in the low 10^{-10} Torr range. The sapphire substrates were cleaned in methanol before loading into the introduction chamber, then sputtered with Ar^+ ions (1.5 keV) for 30 min, and annealed at 1000 °C for 12 h before deposition.

Ni and Co were deposited using two independent electron guns with computer-controlled pneumatic shutters. The thickness of the deposited material was monitored by two calibrated electron impact emission spectroscopy sensors. The evaporation rates were fixed at $\sim$ 0.1 Å/s for Ni and $\sim$ 0.05 Å/s for Co. During growth, the pressure in the vacuum chamber did not exceed 5×10^{-9} Torr. Before deposition of the superlattice, a 50–80 Å Co buffer layer was deposited at 350 °C. The Ni/Co superlattices were grown at 150 °C on these buffer layers, with the substrate continuously rotating around an axis parallel to its surface normal. The number of periods was adjusted so that the total thickness was always approximately 1000 Å.

Figure 1(a) shows the LEED pattern taken after the growth of an $\sim$ 80 Å thick Co buffer layer. In its simplest interpretation, LEED provides information about the structure of the surface, in particular the geometry and

size of the surface unit cell. It has been reported[13] that thin Co films grow in the fcc structure on $Al_2O_3(11\bar{2}0)$, with $Co(111) \parallel Al_2O_3(11\bar{2}0)$ and $Co(110) \parallel Al_2O_3(0001)$. If the Co layer were single domain with a fcc structure, the LEED pattern would show threefold symmetry, that is, three spots at 120° would appear for a given electron-beam energy. However, the measured diffraction pattern shows 12 spots, with approximately the same intensity, at all energies. A closer examination indicates two distinct sets of spots with six spots each. Within one set, all the spots are separated 60° with respect to each other, but one set is rotated 32° with respect to the other. This LEED pattern can be explained by assuming the existence of four different types of fcc domains, two of them rotated 32° with respect to each other, and the other two being 180° twins of these two. Also, it can be easily seen that not all the spots are equivalent, but the width of the spots in one set is significantly smaller than in the other, indicating a correspondingly smaller in-plane mosaic character for this type of domain.

The symmetry, shape, and relative intensities in the LEED patterns taken halfway through [Fig. 1(b)] and after the completion of a $(Ni_{42}/Co_{18})_{16}$ superlattice [Fig. 1(c)] are very similar to that of the buffer layer, indicating that the epitaxial relationship between the buffer layer and the substrate holds throughout the whole superlattice thickness, and that in-plane crystallinity is maintained across the superlattice.

The samples were further characterized *ex situ* with Cu $K\alpha$ radiation ($\lambda = 1.5418$ Å) using a 12 kW rotating anode Rigaku x-ray diffractometer. Different diffraction geometries were used to determine the structural properties (lattice parameter, grain size, mosaic character) in different directions in real space (see Fig. 2).

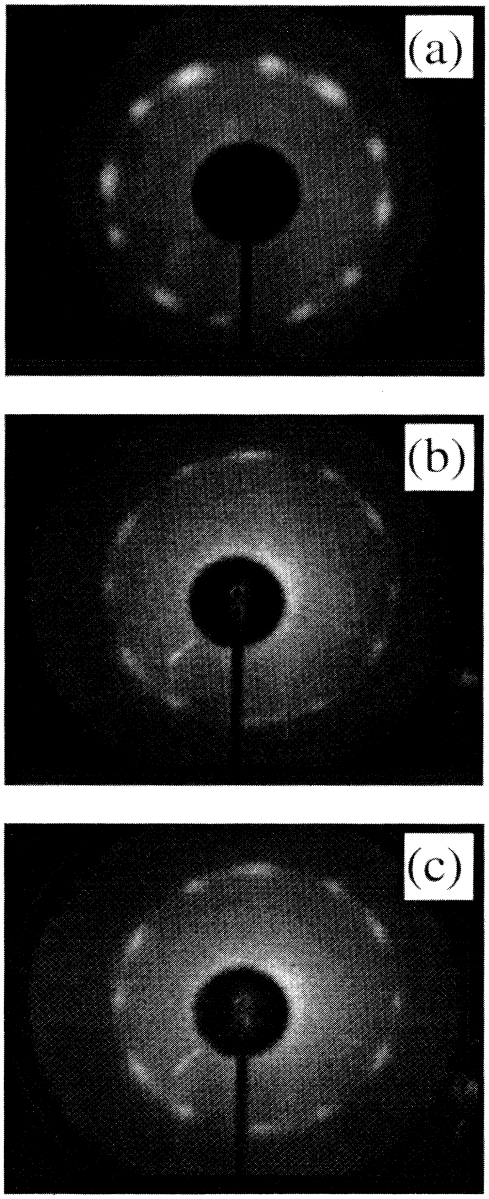

FIG. 1. (a) LEED pattern after deposition of an 80 Å thick Co buffer layer on $Al_2O_3(11\bar{2}0)$ at 350 °C. The primary beam energy is $E_p = 177$ eV. (b) LEED pattern after deposition of the eighth period of a $(Ni_{42}/Co_{18})_{16}$ superlattice. $E_p = 154$ eV. (c) LEED pattern after completion of the $(Ni_{42}/Co_{18})_{16}$ superlattice. $E_p = 169$ eV.

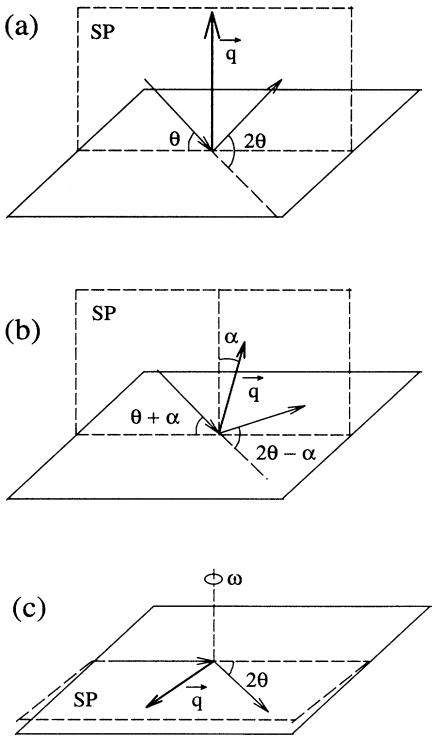

FIG. 2. The different scattering geometries used in x-ray diffraction. In the normal θ-2θ geometry (a), both the scattering plane (SP) and the scattering vector ($\vec{q}$) are normal to the sample surface, giving information about the structural parameters in the growth direction. In (b), the scattering plane is normal to the surface, but the scattering vector is at an angle α with respect to the normal. In (c), both the scattering plane and the scattering vector are almost parallel to the sample surface, giving information about the in-plane structure of the superlattice.

Typical θ-2θ low-angle x-ray diffraction spectra are shown in Fig. 3 for a set of samples with $a = 42$ Å and different Co thicknesses. All spectra show well-defined finite-size peaks, whose separation is related to the total thickness of the multilayer, and superlattice peaks, which result from the new modulation length $\Lambda = a + b$ introduced by the superlattice structure. A detailed quantitative analysis of these spectra is difficult due to the low scattering contrast between Ni and Co, which does not allow for a unique determination of parameters using a structural refinement.[14] Nevertheless, the fact that up to fifth order superlattice and well-defined finite-size peaks are observed in most spectra indicates an approximately square chemical modulation wavelength, with little interdiffusion between the Ni and Co layers.

Auger spectra taken *in situ* during growth confirm these conclusions and give a quantitative estimate for the upper limit of the interdiffused region at the Ni/Co interface. A surface analysis technique, Auger electron spectroscopy gives information about the chemical composition close to the topmost surface layers within the Auger electrons' escape depth. Figure 4(a) shows the high-energy Auger spectra taken after depositing a 59 Å thick Co buffer layer on the sapphire substrate. The three peaks at 656, 716, and 775 eV correspond to *LMM* Co Auger transitions. After deposition of ≈ 4.3 Å of Ni on this buffer layer [Fig. 4(b)], a new peak appears at 848 eV, while the intensity of the peak at 656 eV decreases noticeably. This Co Auger transition is barely visible when the Ni layer thickness increases to ≈ 8.6 Å [Fig. 4(c)], and disappears completely for a Ni thickness of ≈ 12.9 Å. The spectrum in Fig. 4(d) shows only peaks at 716, 783, and 848 eV, which correspond to the *LMM* Auger transitions of pure Ni.

Even after the deposition of several bilayers, which could in principle increase the cumulative surface roughness and consequently the interface disorder, the high-energy Ni and Co Auger transitions almost completely disappear when the overlayer thickness is ≥ 18 Å. Taking into account the escape depth of these Auger electrons [$\sim$ 8-12 Å (Ref. 15)], an upper limit of 4–5 Å can be estimated for the thickness of the interdiffused region, thus confirming the x-ray data and proving the relative sharpness of the Ni/Co interface.

The high-angle θ-2θ x-ray spectra are reproduced in Fig. 5. The peaks at $2\theta \sim 44.5°$ are the central Bragg peaks of the superlattices,[16] corresponding to a weighted average of Ni and Co, probably Ni(111) and either

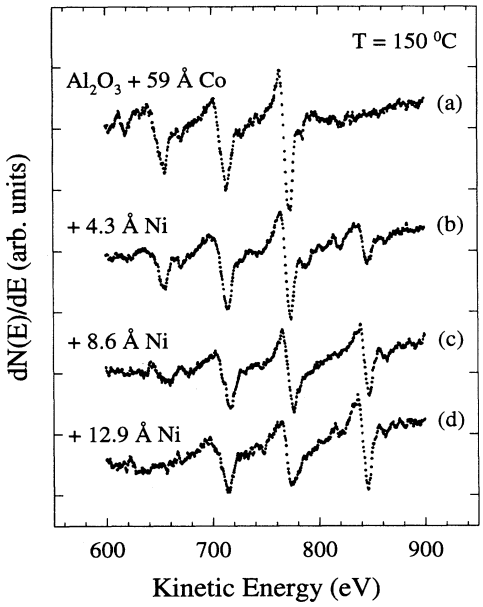

FIG. 4. High-energy Auger spectra taken during the deposition of Ni on a 59 Å thick Co buffer layer.

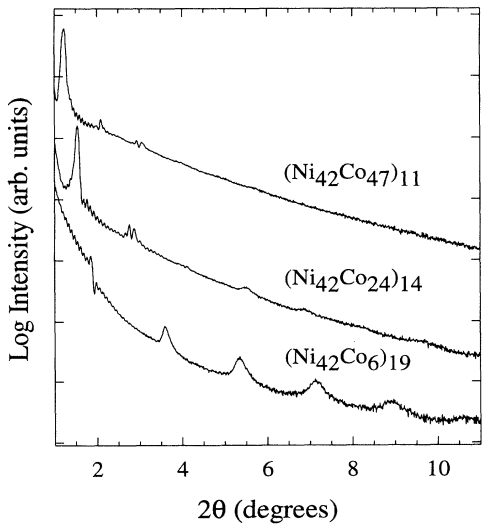

FIG. 3. Low-angle x-ray diffraction spectra for a series of Ni/Co superlattices with a Ni thickness of 42 Å and different (6, 24, and 47 Å) Co thicknesses.

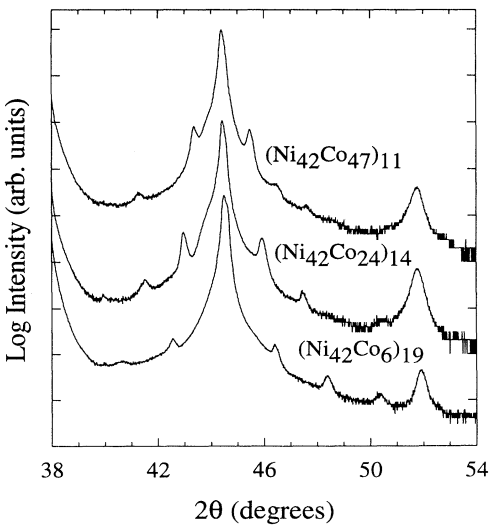

FIG. 5. High-angle x-ray diffraction spectra for a series of Ni/Co superlattices with a Ni thickness of 42 Å and different (6, 24, and 47 Å) Co thicknesses.

Co(0002) or Co(111), depending on whether Co grows in the hcp or fcc structure. The tail at the left side of the spectrum is due to the $(11\bar{2}0)$ reflection of the sapphire substrate, and the peak at $\sim 51.6°$ is due to a small quantity (in all the grown samples less than 1%) of (100) oriented grains. The other peaks shown in the spectra are satellite peaks due to the superlattice periodicity.

The crystalline coherence length $\xi_\perp$ along the (111) direction can be extracted from the widths of the main superlattice x-ray peaks using Scherrer's equation

$$\xi_\perp = \frac{0.9\lambda}{\Delta(2\theta)\cos\theta}, \quad (1)$$

where $\Delta(2\theta)$ is the full width at half maximum (FWHM), θ the peak position, and λ the x-ray wavelength. For all of the grown superlattices, $\Delta(2\theta)$ ranges from 0.09° to 0.13°, which gives a crystalline coherence length ranging between 650 and 950 Å, and thus is in most cases almost equal to the whole superlattice thickness. This also confirms the LEED data that showed that the superlattices are single crystalline in the growth direction. No correlation was found between the coherence length and the Ni and Co thickness, indicating that the small variations are due to an uncontrolled parameter, such as the structural quality of the Co buffer layer.

Transverse scans across the fundamental (111) Bragg peaks (rocking curves) give information about the out-of-plane mosaic character. In our samples, the widths of the rocking curves, which have almost purely Gaussian shapes, range between 0.3° and 1°, again with no correlation with the modulation wavelength or the Ni and Co layer thicknesses.

Figure 6(a) shows the evolution of the average lattice parameter in the (111) direction (parallel to the surface normal) obtained from the position of the main superlattice peak for a series of Ni/Co superlattices with $a = 42$ Å as a function of the Co thickness. The solid line is the theoretical lattice parameter obtained as a weighted average of the (111) Ni [$d_{\mathrm{Ni}}(111) = 2.0332$ Å] and Co fcc [$d^{fcc}_{\mathrm{Co}}(111) = 2.0467$ Å] lattice parameters while the dashed line is the predicted value if Co grew in the hcp structure [$d^{hcp}_{\mathrm{Co}}(0002) = 2.0230$ Å]. The data show that Co has a lattice parameter close to that of bulk fcc Co in the (111) direction, even for Co layers as thick as 120 Å. The dotted line is a least squares fit to the experimental points with the Co lattice parameter as the fitting parameter. This fit gives $d_{\mathrm{Co}}(111) = 2.0450$ Å, which agrees with the bulk fcc Co lattice parameter within 0.08%.

As the superlattices are lattice matched in plane (see below), an attempt was made to fit the experimental data taking into account the predicted Poisson response perpendicular to the layers,[17] using the known elastic constants of bulk Ni and fcc Co. However, no agreement was found. This seems to prove that, like other metallic superlattices,[18] Ni/Co superlattices do not show the Poisson effect predicted by the standard elasticity theory.

These data, however, only measure the lattice parameter in the growth direction, but give no information about the stacking sequence. A further clue about the Co structure can be obtained by measuring the average lattice parameter in other crystallographic directions. Using

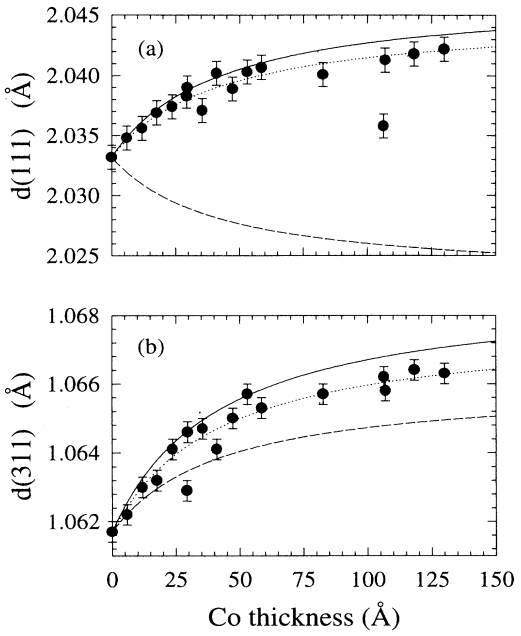

FIG. 6. Evolution of the average (111) and (311) lattice parameters as a function of the Co thickness in a series of superlattices with constant (42 Å) Ni thickness. The solid line is obtained as a weighted average of the Ni and Co fcc lattice parameters, while the dashed line is the weighted average of the corresponding Ni and Co hcp lattice parameters. The dotted line is a least squares fit to the experimental points with the Co lattice parameter as the fitting variable.

an x-ray diffraction geometry with the scattering vector at 29.3° with respect to the surface normal [Fig. 2(b)], we measured the lattice parameter in the (311) direction for the same set of samples. The results are shown in Fig. 6(b). In this graph, the solid line is the theoretical lattice parameter obtained as a weighted average of the (311) Ni and Co fcc lattice parameters, while the dashed line is obtained as a weighted average of the (311) Ni and $(11\bar{2}2)$ Co hcp lattice parameters. As in Fig. 6(a), the experimental lattice parameter agrees better with the one predicted for the Co fcc structure. The least squares fit to the experimental points (dotted line) gives $d_{\mathrm{Co}}(311) = 1.0678$ Å, again $\sim 0.09\%$ smaller than the bulk Co fcc lattice parameter.

This implies that, when $a = 42$ Å, Co grows in the fcc structure even for Co layer thicknesses as large as 120 Å. The lattice parameters measured in the (111) and (311) directions seem to indicate, however, a small contraction (0.08%) with respect to bulk fcc Co.

The fcc structure of Co can also be stabilized with thinner Ni layers. Figure 7 shows the average lattice parameters measured in the (111) and (311) directions for a series of superlattices where the Ni thickness is $a = 22$ Å. The excellent agreement with the predicted values shows that, also in this case, Co grows in the fcc structure even up to a thickness of 60 Å.

Grazing incidence x-ray spectra [Fig. 2(c)], with the film plane almost parallel to the scattering plane, as

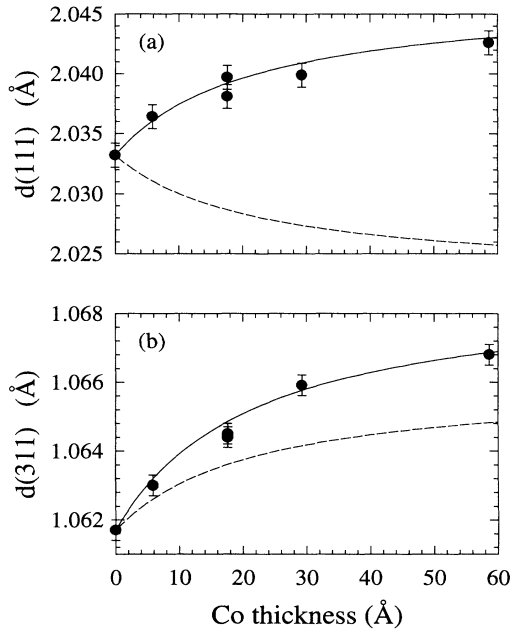

FIG. 7. Evolution of the average (111) and (311) lattice parameters as a function of the Co thickness in a series of superlattices with constant (22 Å) Ni thickness. The solid line is obtained as a weighted average of the Ni and Co fcc lattice parameters, while the dashed line is the weighted average of the corresponding Ni and Co hcp lattice parameters.

shown in Fig. 8 for a $(Ni_{42}/Co_{35})_{13}$ superlattice, allow the determination of the epitaxial relationship between the superlattice and the sapphire substrate. Twelve {220} reflections, equivalent to the 12 spots present in the LEED patterns in Fig. 2, are clearly observed when turning the sample around the surface normal with the detector fixed at $2\theta = 76.5°$, reflecting the in-plane symmetry of the superlattice. The sharp peaks (marked with $*$) at 52.4° and 72.4° are reflections of the sapphire substrate. In particular, the peak at 72.4° corresponds to the $(\bar{1}10\ 10)$ Bragg peak, and allows a determination of the absolute position of the {220} superlattice peaks with respect to the substrate. In this way, the following epitaxial relationships can be obtained for the four different types of domains:

(a) Ni/Co[110] || $Al_2O_3[\bar{1}100]$,
(b) Ni/Co[110] || $Al_2O_3[\bar{1}10\bar{2}]$,
(c) Ni/Co[11$\bar{2}$] || $Al_2O_3[\bar{1}100]$, and
(d) Ni/Co[11$\bar{2}$] || $Al_2O_3[\bar{1}10\bar{2}]$.

Thus, one type of domain aligns one [220] vector with the $[\bar{1}100]$ direction of sapphire, while the other one aligns itself with the $[\bar{1}10\bar{2}]$ direction, which is rotated $\sim 32°$ with respect to the first one. As mentioned above, the other two types of domains are 180° twins of these two (see Fig. 9).

Figure 10 shows a contour plot of these grazing angle incidence scans for different values of the detector angle around a particular (220) in-plane Bragg peak. The fact that the peak has clearly only one component, with a maximum around $2\theta = 76.25°$ [halfway between the expected positions for pure Co (75.85°) and Ni (76.50°)], indicates that the superlattices are lattice matched in the plane.

The in-plane mosaic character, grain size, and lattice parameter of the superlattice can be directly obtained from these types of scans. The in-plane lattice parameters measured in this way are shown in Fig. 11 as functions of the Co thickness for a series of superlattices with a fixed at 42 Å. The common in-plane lattice parameter is thus approximately a weighted average of the Ni and Co lattice parameters. The mosaic character, obtained from a transverse scan across the (220) Bragg peaks for

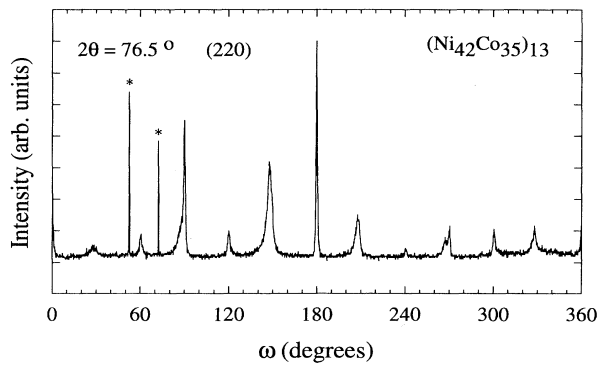

FIG. 8. Grazing angle x-ray diffraction spectra for a $(Ni_{42}/Co_{18})_{16}$ superlattice. The scattering plane is almost parallel to the sample surface, and the sample was rotated around the surface normal with the detector fixed at $2\theta = 76.5°$, corresponding to the (220) in-plane lattice parameter of the superlattice. The peaks at 52.4° and 72.4° (marked with $*$) are reflections from the sapphire substrate.

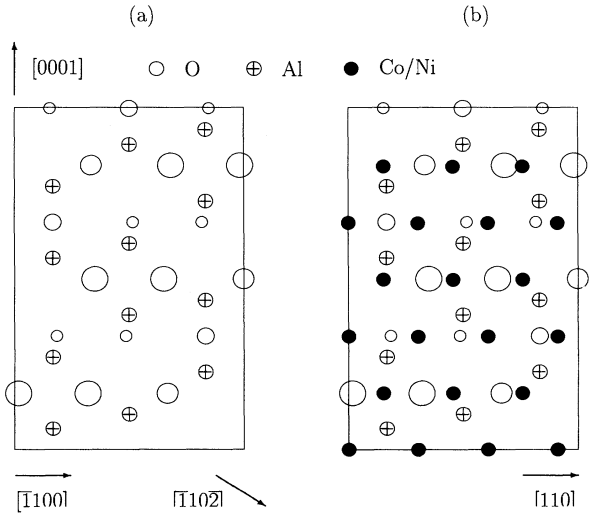

FIG. 9. The epitaxial relationship for Co/Ni superlattices on $Al_2O_3(11\bar{2}0)$: (a) surface unit cell of the sapphire substrate; (b) for type (a) domains, Ni/Co[110] || $Al_2O_3[\bar{1}100]$. Type (b) domains can be obtained by rotating the superlattice unit cell $\sim 32°$ in the clockwise direction around an axis parallel to the surface normal, so that Ni/Co[110] || $Al_2O_3[\bar{1}10\bar{2}]$. Domains type (c) and (d) are 180° twins of these two.

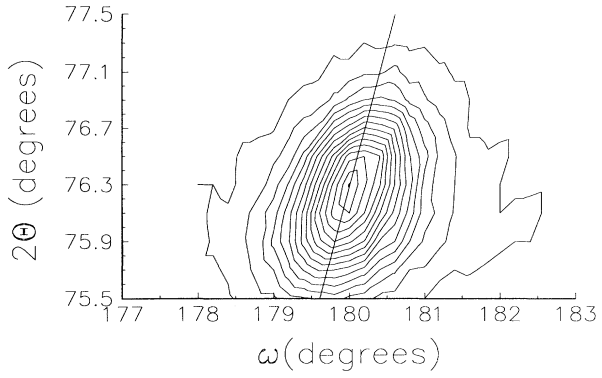

FIG. 10. Contour plot taken from grazing angle x-ray diffraction spectra for a $(Ni_{42}/Co_{18})_{16}$ superlattice for different values of the detector angle. The straight line shows the direction of a θ-2θ scan.

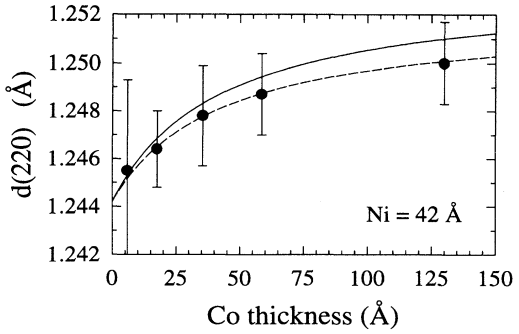

FIG. 11. Evolution of the average (220) lattice parameter as a function of the Co thickness in a series of superlattices with constant (42 Å) Ni thickness. The solid line is obtained as a weighted average of the Ni and Co fcc lattice parameters, while the dashed line is the weighted average of the corresponding Ni and Co hcp lattice parameters.

2θ = constant, is typically 1° for domains type (a) and (c), and 3° for domains type (b) and (d). The in-plane domain size, as obtained from the FWHM of θ-2θ scans along the Bragg peak, ranges between 100 and 200 Å.

In conclusion, the structure of Ni/Co(111) superlattices of almost square chemical modulation has been characterized with a combination of surface analysis techniques and x-ray diffraction. We have shown that these superlattices grow quasiepitaxially (i.e., are single crystalline in the growth direction but show four different types of in-plane domains) on sapphire substrates, with both Ni and Co growing in the fcc structure, even for superlattices where the Ni thickness is 22 Å and smaller than the Co thickness. The superlattices are in-plane lattice matched, and exhibit the bulk lattice parameters in the growth direction, contrary to expectations based on their Poisson ratio.

This work was supported by the U.S. National Science Foundation and the Department of Energy. J.M.G. is grateful for the support provided by the Spanish Secretaría de Estado de Universidades e Investigación.

[1] L. Falicov, D. T. Pierce, S. D. Bader, K. B. Hathaway, H. J. Hopster, D. N. Lambeth, S. S. P. Parkin, G. Prinz, M. Salamon, I. K. Schuller, and R. H. Victora, J. Mater. Res. **5**, 1299 (1990).

[2] *Physics and Applications of Multilayered Structures*, edited by P. Dhez and C. Weisbuch (Plenum Publishing Co., New York, 1988).

[3] *Metallic Superlattices: Artificially Structured Materials*, edited by T. Shinjo and T. Takada (Elsevier, Amsterdam, 1987).

[4] M. N. Baibich, J. M. Broto, A. Fert, F. Nguyen van Dau, F. Petroff, P. E. Etienne, G. Creuzet, A. Friedrich, and J. Chazelas, Phys. Rev. Lett. **61**, 2472 (1988).

[5] S. S. P. Parkin, Phys. Rev. Lett. **64**, 2304 (1990).

[6] P. F. Carcia, A. D. Meinholdt, and A. Suna, Appl. Phys. Lett. **47**, 178 (1985).

[7] J. M. Gallego, D. Lederman, and I. K. Schuller (unpublished).

[8] J. M. Gallego, D. Lederman, T. J. Moran, and I. K. Schuller, Appl. Phys. Lett. **64**, 2590 (1994).

[9] G. H. O. Daalderop, P. J. Kelly, and F. J. A. den Broeder, Phys. Rev. Lett. **68**, 682 (1992).

[10] M. Komuro, Y. Kozono, S. Narishige, M. Hanazono, and Y. Sugita, Jpn. J. Appl. Phys. **27**, L2105 (1988).

[11] A. S. Edelstein, C. Kim, S. B. Qadri, K. H. Kim, V. Browning, H. Y. Yu, B. Maruyama, and R. K. Everett, Solid State Commun. **76**, 1379 (1990).

[12] P. J. H. Bloemen, W. J. M. de Jonge, and F. J. A. den Broeder, J. Appl. Phys. **72**, 4840 (1992).

[13] Ch. Morawe, A. Stierle, N. Metoki, K. Bröhl, and H. Zabel, J. Magn. Magn. Mater. **102**, 223 (1991).

[14] E. E. Fullerton, I. K. Schuller, H. Vanderstraeten, and Y. Bruynseraede, Phys. Rev. B **45**, 9292 (1992).

[15] M. P. Seah and W. A. Dench, Surf. Interface Anal. **1**, 2 (1979).

[16] I. K. Schuller, Phys. Rev. Lett. **44**, 1597 (1980).

[17] P. Bödeker, A. Abromeit, K. Bröhl, P. Sonntag, N. Metoki, and H. Zabel, Phys. Rev. B **47**, 2353 (1993).

[18] A. Fartash, M. Grimsditch, E. E. Fullerton, and I. K. Schuller, Phys. Rev. B **47**, 12 813 (1993).

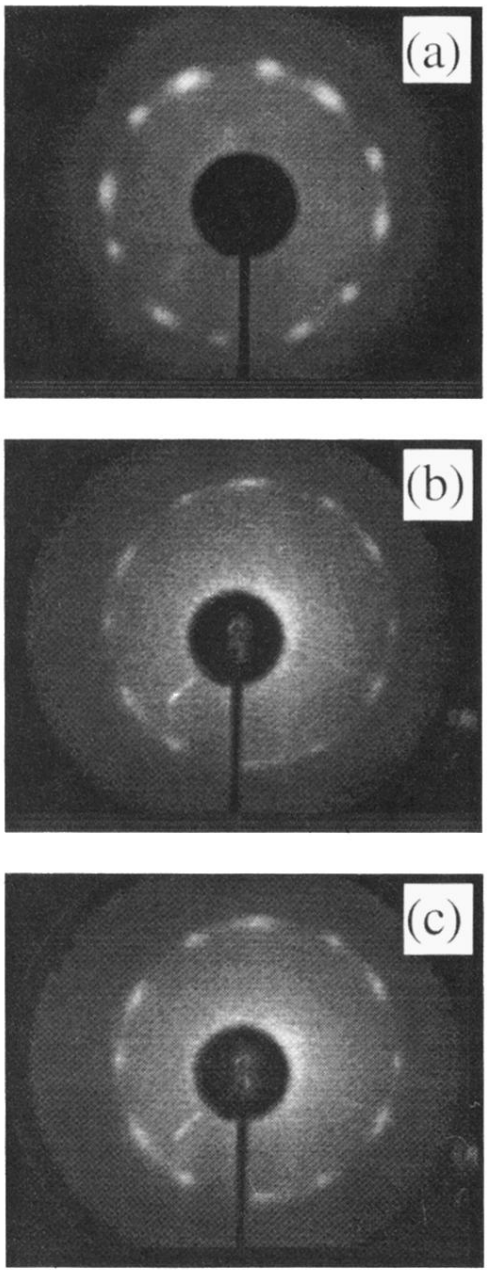

FIG. 1. (a) LEED pattern after deposition of an 80 Å thick Co buffer layer on $Al_2O_3(11\bar{2}0)$ at 350 °C. The primary beam energy is $E_p = 177$ eV. (b) LEED pattern after deposition of the eighth period of a $(Ni_{42}/Co_{18})_{16}$ superlattice. $E_p = 154$ eV. (c) LEED pattern after completion of the $(Ni_{42}/Co_{18})_{16}$ superlattice. $E_p = 169$ eV.